universe

IMPACT FACTOR 2.813

CITESCORE 3.2

Article

Scalar Particles around a Rindler–Schwarzschild Wormhole

C. R. Muniz, H. R. Christiansen, M. S. Cunha, J. Furtado and V. B. Bezerra

MDPI

https://doi.org/10.3390/universe8120616

universe

MDPI

Article

Scalar Particles around a Rindler–Schwarzschild Wormhole

C. R. Muniz [1], H. R. Christiansen [2,*], M. S. Cunha [3], J. Furtado [4] and V. B. Bezerra [5]

[1] Departamento de Física, FECLI, Universidade Estadual do Ceará, Av. Dário Rabelo, Iguatu 63500-518, Brazil
[2] Departamento de Física, Instituto Federal de Ciências, Educação e Tecnologia, IFCE, Campus Maranguape, Maranguape 61940-750, Brazil
[3] Departamento de Física, CCT, Universidade Estadual do Ceará, Fortaleza 60714-903, Brazil
[4] Departamento de Física, CCT, Universidade Federal do Cariri, Juazeiro do Norte 63048-080, Brazil
[5] Departamento de Física, CCEN, Universidade Federal da Paraíba, C.P. 5008, João Pessoa 58051-970, Brazil
* Correspondence: hugo.christiansen@ifce.edu.br

Abstract: In this paper, we study quantum relativistic features of a scalar field around the Rindler–Schwarzschild wormhole. First, we introduce this new class of spacetime, investigating some energy conditions and verifying their violation in a region nearby the wormhole throat, which means that the object must have an exotic energy in order to prevent its collapse. Then, we study the behavior of the massless scalar field in this spacetime and compute the effective potential by means of tortoise coordinates. We show that such a potential is attractive close to the throat and that it is traversable via quantum tunneling by massive particles with sufficiently low energies. The solution of the Klein–Gordon equation is obtained subsequently, showing that the energy spectrum of the field is subject to a constraint, which induces a decreasing oscillatory behavior. By imposing Dirichlet boundary conditions on a spherical shell in the neighborhood of the throat we can determine the particle energy levels, and we use this spectrum to calculate the quantum revival of the eigenstates. Finally, we compute the Casimir energy associated with the massless scalar field at zero temperature. We perform this calculation by means of the sum of the modes method. The zero-point energy is regularized using the Epstein–Hurwitz zeta-function. We also obtain an analytical expression for the Casimir force acting on the shell.

Keywords: wormholes; general relativity; scalar fields; Casimir effect; Rindler space

Citation: Muniz, C.R.; Christiansen, H.R.; Cunha, M.S.; Furtado, J.; Bezerra, V.B. Scalar Particles around a Rindler–Schwarzschild Wormhole. *Universe* **2022**, *8*, 616. https://doi.org/10.3390/universe8120616

Academic Editor: Maxim Chernodub

Received: 18 October 2022
Accepted: 22 November 2022
Published: 24 November 2022

1. Introduction

Wormholes are hypothetical topologically non-trivial spacetime objects connecting arbitrarily distant regions of the universe, or even different universes. These structures, although not predicted by general relativity (GR), are viable solutions of Einstein equations in GR and in many extended theories of gravity. The term wormhole, in fact, was coined [1] more than two decades after the first vacuum solution, the so-called Einstein–Rosen bridge [2], was found. Later on, it was shown that this type of wormhole is unstable if it connects two parts of the same universe, collapsing too quickly for any particle (even light) to pass from one side to the other [3]. Solutions corresponding to traversable wormholes were found in 1973 by Bronnikov and Ellis [4,5] and became well-known after the papers of Morris, Thorne, and Visser [6–8].

The throat of a wormhole is in principle unstable to small perturbations and collapses under its own mass gravity. In brane models, negative pressure can be obtained from the brane tension. Such models assume that our universe is a (3 + 1)-dimensional subspace embedded in a higher-dimensional bulk space. The brane can bend hard enough to make space points far apart on the brane be close in the bulk and thereafter be potentially connected through a wormhole. If we assume the presence of a BH on each side, against their gravitational attraction there will be the repulsion between folds due to the brane tension. Brane tension thus compensates the demand for exotic matter [9]. Another way to balance gravity is to place the structure in a de Sitter background [10].

Traversable wormholes generally require the input of exotic sources of negative energy in order to avoid the collapse [11]. In extended theories of gravity, wormholes may exist even without exotic matter and even without matter, see for instance Refs. [12–15]. Fortunately, an arbitrarily thin layer of negative energy density is sufficient to keep a macroscopic wormhole stable [16]. Negative energy density can for instance be produced by Casimir forces [17]. Indeed, the Casimir effect has been proved to occur among ordinary matter pieces of diverse shapes and materials [18–20]. The nature of this effect, as originally pointed out, is connected with the zero-point energy of the quantum (electrodynamical) vacuum distorted by parallel plates and depends strongly on the geometry of the boundaries. In Ref. [6] it was shown that the plates separation should be smaller than the electron Compton wavelength so that the physical device cannot be realized. Later, it was concluded that the mass of the plates compensate for the negative energy density, and the traversable wormhole is not completed [21,22]. Recently, Garattini [23] called attention to the fact that nothing was said about the possible forms of the shape function and the redshift function in the literature. These functions are related when imposing an equation of state among radial pressure and energy density $p_r = \varpi\rho$. For $\varpi = 3$ one meets the conserved Casimir stress energy tensor (contributing only at the Planck scale); for $\varpi = 1$ the Ellis–Bronnikov wormhole (of sub-planckian size), $\varpi = -1$ is for ordinary vacuum and $\varpi < -1$ for phantom energy (see e.g., [24]).

The actual existence of traversable wormholes is allowed in GR if quantum effects are included. Indeed, during the quantum gravity phase of the primordial universe, large quantum fluctuations in the geometry and topology of spacetime could likely give rise to such structures and provide the negative energy density necessary to stabilize them. Although microscopic, such primordial quantum configurations could be made macroscopic during expansion and thus potentially observable [25]. The potential existence of astrophysical wormholes is discussed in Ref. [26]. Nowadays, technological devices are at the edge of providing evidence about some astrophysical black holes being actually the mouths of physical wormholes, see e.g., [27,28].

In the next section, we introduce the the Rindler–Schwarzschild wormhole metric that we will consider throughout this paper, and we will discuss the violation of Null and Average Null Energy Conditions around it. In Section 3 we analyze the equation of motion of a scalar field surrounding the wormhole spacetime and obtain its spectrum and solutions considering the appropriated boundary conditions. In Section 4 we compute the quantum revival of the wave function. Section 5 is dedicated to the calculation of the Casimir energy of the scalar field in the wormhole for a thin spherical shell close to the throat. In the final section we present our conclusions.

2. Metric and Energy Conditions

The first wormhole solution was originally constructed after the static black hole spherically symmetric Schwarzschild solution [2]. This metric contains two asymptotically flat spacetimes, $r > 2$ GM and $r < 2$ GM. These are two disconnected spacetimes sharing the same horizon at the $r = 2$ GM hypersurface. The existence of an event horizon prevents such a wormhole from being traversable. One makes it traversable by copying the space given by $r > 2$ GM and then pasting the two copies together. In this representation, the wormhole does not connect separate points of the same universe but two different universes; each one with its own black hole, infinitely distant from the other.

We introduce a novel wormhole spacetime that asymptotically behaves as a non-flat Rindler-like spacetime given by

$$ds^2 = \alpha^q r^q dt^2 - \frac{dr^2}{1 - b(r)/r} - r^2 d\Omega^2, \tag{1}$$

where $b(r)$ is the shape function. The usual Rindler spacetime, recovered for $q = 2$ and large r, is the coordinate frame of an observer undergoing constant proper acceleration in an otherwise flat Minkowski spacetime [29]. Note that while we assume a Schwarzschild-like

g_{rr} we replace g_{tt} by a Rindler type function. Thus, we will henceforth consider that the shape function has the form $b(r) = 2\,\mathrm{GM} \equiv b_0$, where b_0 is the throat radius. The Ricci scalar curvature associated to the metric (1) is given by

$$R_S = -\frac{q[q(r-b_0)+b_0-2r]}{2r^3}. \tag{2}$$

Differently from the Rindler–Ellis–Bronnikov wormhole [30], this curvature depends manifestly on the throat radius, except for $q = 1$.

By calculating the Einstein tensor in the frame basis and defining the energy momentum $T_{\mu\nu} = (1/\kappa)G_{\mu\nu}$, with $T_{00} = \rho$, $T_{11} = p_r$, $T_{22} = p_\theta = T_{33} = p_\phi$, one can arrive at the Null Energy Conditions (NEC) for the perfect fluid that generates the wormhole. Such conditions for the Rindler–Schwarzschild wormhole are violated in a finite region nearby the throat. Indeed,

$$\begin{aligned} \rho \quad + \quad p_r &= \frac{2r-3b_0}{r^3} < 0 \text{ in the interval } b_0 \leq r < \frac{3}{2}b_0, \\ \rho \quad + \quad p_\phi (= p_\theta) &= \frac{1}{r^2} \geq 0 \text{ for all } r, \end{aligned} \tag{3}$$

with ρ and p_r being the energy density and radial pressure, respectively, and p_ϕ, p_θ the lateral pressures. Such a violation in NEC occurs in a region slightly larger than the one corresponding to the Rindler–Ellis–Bronnikov wormhole. The object under consideration here can be thought of as being sustained by two fluids, an exotic-type and another that satisfies NEC, in accordance with Ref. [30]. Taking into account the generalized Rindler–Ellis–Bronnikov wormhole, with shape function given by $b(r) = r - r^{3-2m}(r^m - b_0^m)^{2-2/m}$ ($m \geq 2$ is an even integer [31], noting that $m = 2$ yields the usual Ellis–Bronnikov wormhole), we have that for $m \geq 4$ the referred violation occurs in a region even smaller since this region now corresponds to the interval $b_0 \leq r < m^{1/m}b_0$.

Regarding the Averaged Null Energy Conditions (ANEC) $\int T_{\mu\nu}k^\mu k^\nu d\lambda \geq 0$, there is again a violation. ANEC must be calculated along the radial null geodesics and result in

$$\frac{1}{\kappa\alpha}\int_{b_0}^{\infty}\frac{2r-3b_0}{r^3\sqrt{r(r-b_0)}}dr = -\frac{8}{15\kappa\alpha b_0^2}. \tag{4}$$

Note however that, by fixing α, this violation can be neglected for large wormhole throats (i.e., for macroscopic deformed Schwarzschild-like wormholes). In fact, such a violation is smaller than the one obtained for the wormhole discussed in Ref. [30].

3. Massless Scalar Field and Energy Levels

We will consider the radial part of the Klein–Gordon equation, $\frac{1}{\sqrt{-g}}\partial_\mu[\sqrt{-g}g^{\mu\nu}\partial_\nu\phi] + m^2\phi = 0$, for a scalar field with profile $\phi(r,\theta,\varphi,t) = \exp(-i\omega t)Y_\ell^k(\theta,\varphi)R(r)$ (k is the azimuthal quantum number) placed in the spacetime given by Equation (1). Our main focus here will be on the massless field but for the sake of completeness we will also consider massive particles in some calculations. Performing the transformation $R(r) = \xi(r)\sqrt{g_{rr}}/r$, we obtain an equation for $\xi(r)$ which turns to be a Schrödinger-type equation on introducing the tortoise radial coordinate, r_*, as follows

$$\frac{dr_*}{dr} = \sqrt{-\frac{g_{rr}}{g_{00}}} = \alpha^{-q/2}r^{-q/2}\left(1-\frac{b_0}{r}\right)^{-1/2}. \tag{5}$$

The coordinate transformation above allows us to map the defined positive radial coordinate r into $-\infty < r_* < \infty$, in order to include both the foils ($r_* > 0$ and $r_* < 0$) joined by the wormhole throat. Thus, the "inner" ("outer") space of the Schwarzschild-like sector, $0 < r < b_0$ ($r > b_0$), is mapped into $-\infty < r_* < 0$ ($r_* > 0$). For $q = 2$ we have

$$r = \frac{1}{4} b_0 e^{-\alpha r_*} (1 + e^{\alpha r_*})^2, \tag{6}$$

so that at the wormhole throat, $r = b_0$, $r_* = 0$. The Schrödinger-type equation is given by,

$$-\frac{d^2\xi(r)}{dr_*^2} + \left[V_{eff}(r) - \omega^2\right]\xi(r) = 0, \tag{7}$$

where the effective potential is

$$V_{eff} = \frac{\alpha^2\left\{b_0^2 + 4b_0\left[(2\ell+1)^2 r - 4m^2 r^3\right] - 4r^2\left[4\ell(\ell+1) - 4m^2 r^2 + 1\right]\right\}}{16r(b_0 - r)}, \tag{8}$$

In Figure 1, we show the potential resulting from the Rindler–Schwarzschild wormhole in terms of the tortoise coordinate for both massive and massless scalar particles. Nearby the wormhole throat, the effective potential is attractive and falls as $-1/r_*^2$. Notice that for massive particles with low energies, at sufficient distances from the throat there is the possibility of the particle to traverse the wormhole via quantum tunneling.

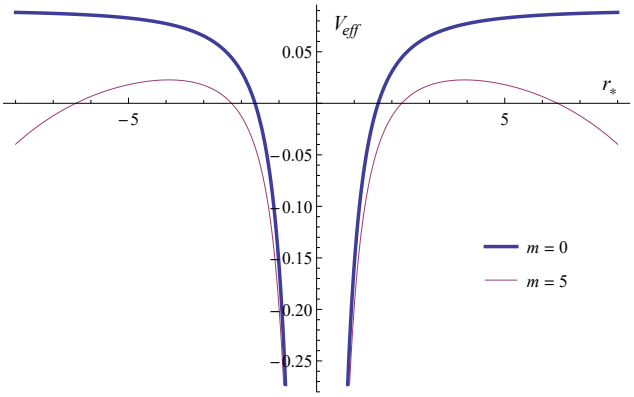

Figure 1. Effective potential for both massive and massless scalar fields around the Rindler–Schwarzschild wormhole ($q = 2$), with $\alpha = 0.2$, $\ell = 1$ and $b_0 = 0.2$ in Planck units.

The solutions of Equation (7) in the Rindler–Schwarzschild wormhole are given in terms of the Legendre functions of first ($P_s(z)$) and second ($Q_s(z)$) types, as follows

$$R(r) = C_1 P_s\left(\frac{2r}{b_0} - 1\right) + C_2 Q_s\left(\frac{2r}{b_0} - 1\right), \tag{9}$$

where $s = \frac{\sqrt{\alpha^2(2\ell+1)^2 - 4\omega^2} - \alpha}{2\alpha}$. Note that $Q_s\left(\frac{2r}{b_0} - 1\right)$ diverges at the throat, $r = b_0$, and then we will take $C_2 = 0$. In Figure 2 we depict the behavior of the $R(r)$ as a function of the radial (left panel) and tortoise (right panel) coordinates, for $C_1 = 1$.

The decreasing oscillatory behavior of the radial function corresponds to a complex s, which is given by $s = -\frac{1}{2} + i\frac{\sqrt{4\omega^2 - \alpha^2(2\ell+1)^2}}{2\alpha}$. This implies the following constraint on the particle energy

$$\omega > \left|\frac{\alpha(2\ell+1)}{2}\right|. \tag{10}$$

We draw attention to the fact that such a behavior of the massless scalar field is the same as discussed in Ref. [30] for the deformed Ellis–Bronnikov wormhole.

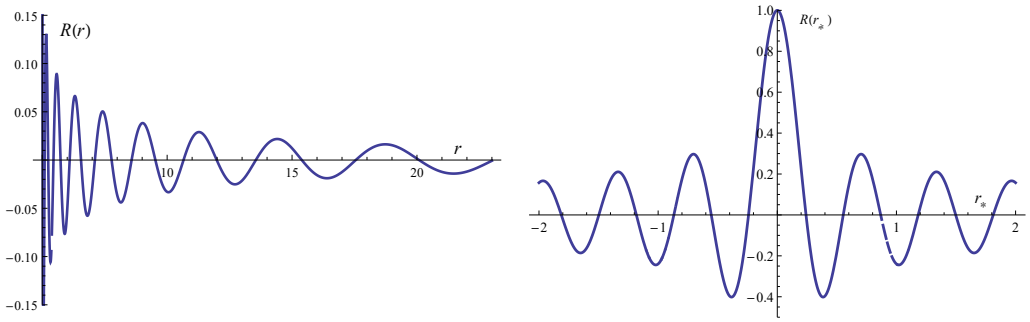

Figure 2. Radial part of the massless scalar field around the deformed Rindler–Schwarzschild wormhole, in terms of the radial coordinate (**left**), and tortoise coordinate (**right**). The parameter settings are $\ell = 1$, $b_0 = 1$, $\alpha = 0.5$, and $\omega = 10$ in Planck units.

We consider now the hypergeometric representation of $P_s(z)$, given by

$$P_s(z) = {}_2F_1(-s; s+1; 1; \frac{1-z}{2}), \tag{11}$$

valid in the interval $1 < z < \infty$. Thus, our radial solution becomes

$$R(r) = C_1\, {}_2F_1\left(\frac{1}{2} - i\lambda; -\frac{1}{2} + i\lambda; 1; 1 - \frac{r}{b_0}\right), \tag{12}$$

where we have defined the dimensionless quantity $\lambda = \sqrt{4\omega^2 - \alpha^2(2\ell+1)^2}/2\alpha$. In order to compute some possible energy eigenvalues for a particle in orbit around the wormhole, let us expand Equation (12) around $r = b_0$, up to first order in $(1 - r/b_0)$. In this region, we find

$$R(r) \propto 1 + \left(\lambda^2 + \frac{1}{4}\right)\left(1 - \frac{r}{b_0}\right) + \mathcal{O}\left[\left(1 - \frac{r}{b_0}\right)^2\right]. \tag{13}$$

From now on, we will use a "hard-shell condition", so that nearby the wormhole throat, $r = r_s \approx b_0$, we get $R(r_s) \approx 0$. In fact, for arbitrary high energies, the potential barrier profile approximates the wormhole throat and the energy levels are given by

$$\omega_\ell \approx \alpha\sqrt{\ell(\ell+1) + \frac{b_0}{r_s - b_0}}, \tag{14}$$

which are higher the closer the shell is to the wormhole throat.

4. Quantum Revival Characteristic Time

Quantum revival is said to occur when the wave function recovers its initial state at an instant dubbed revival time. For a particular quantum number ν_i it is defined by

$$\tau = \frac{4\pi}{\left|\left(\frac{\partial^2\omega_\nu}{\partial\nu^2}\right)_{\nu=\nu_i}\right|}. \tag{15}$$

The energy levels obtained in Equation (14) depend on just one quantum number, the polar quantum number ℓ. Thus, for the ℓ eigenstate, the quantum revival is given by

$$\tau \approx \left|\frac{16\pi[(b_0 - r_s)\ell(\ell+1) - b_0]\sqrt{\frac{b_0}{r_s - b_0} + \ell(\ell+1)}}{\alpha(r_s - 5b_0)}\right|. \tag{16}$$

In Figure 3, we depict these characteristic revival times as a function of ℓ for some values of the deformation parameter, α. Notice that the minimum occurs for the null angular momentum, namely, $\ell = 0$, yielding

$$\tau_{min} \approx \left| \frac{16\pi b_0}{\alpha(r_s - 5b_0)} \sqrt{\frac{b_0}{r_s - b_0}} \right|. \tag{17}$$

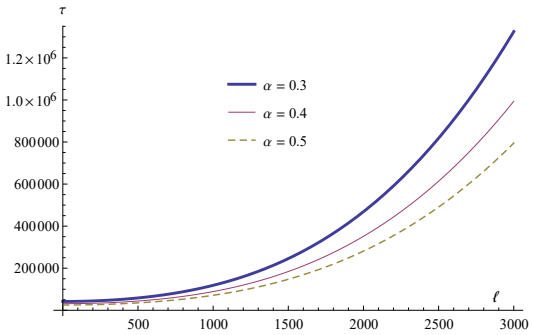

Figure 3. Quantum revival time of the eigenstates of the massless scalar field around the deformed Rindler–Schwarzschild wormhole given in terms of the polar quantum number ℓ, for some values of α, with $b_0 = 1.0$ and $r_s = 1.000001\ b_0$, in Planck units.

5. Casimir Energy and Force

In this section, let us calculate the Casimir energy $\mathcal{E}_C$ of the massless scalar field around the deformed Rindler–Schwarzschild wormhole in the presence of a thin spherical shell nearby the throat. We will do it through a direct summation of the modes. As we have seen previously, the field satisfies the Dirichlet boundary conditions on the shell. We shall adopt a suitable procedure of regularization in order to obtain a finite result. Considering Equation (14) and using the fact that $r_s \approx b_0$, the initial expression for the zero-point energy for the scalar field is given by

$$E_0 = \frac{1}{2}\sum_{\ell=0}^{\infty} g(\ell)\omega_\ell = \alpha \sum_{\ell=0}^{\infty}\left(\ell + \frac{1}{2}\right)\sqrt{\left(\ell + \frac{1}{2}\right)^2 + \frac{b_0}{r_s - b_0} - \frac{1}{4}}, \tag{18}$$

where $g(\ell) = 2\ell + 1$ is the system degeneracy.

In order to regularize the (divergent) zero-point energy we will employ the zeta-function procedure. Before doing this, let us express E_0 in the form [32]

$$E_0 = \frac{\omega_0}{2} + \frac{\alpha}{1-s}\frac{\partial \zeta_{EH}(s-1;a,b)}{\partial a}, \tag{19}$$

where $\zeta_{EH}(s;a,b)$ is the Epstein–Hurwitz zeta-function given by $\zeta_{EH}(s;a,b) = \sum_{n=1}^{\infty}[(n+a)^2 + b]^{-s}$, with $b > 0$. In the present case we have $s = -1/2$, $a = 1/2$, and $b = b_0/(r_s - b_0) - 1/4 \approx b_0/(r_s - b_0)$. The regularization can be seen by using the identity [33]

$$\begin{aligned}\zeta_{EH}(s;a,b) &= \frac{b^{-s}}{\Gamma(s)}\sum_{n=0}^{\infty}\frac{(-1)^n\Gamma(n+s)}{n!}b^{-n}\zeta(-2n,a) + \frac{\sqrt{\pi}\Gamma(s-1/2)}{2\Gamma(s)}b^{1/2-s} \\ &+ \frac{2\pi^s}{\Gamma(s)}b^{1/4-s/2}\sum_{n=1}^{\infty}n^{s-1/2}\cos(2\pi n a)K_{s-1/2}(2\pi n\sqrt{b}),\end{aligned} \tag{20}$$

where $\zeta(p,q)$ is the Hurwitz zeta-function and $K_\mu(z)$ is the Bessel function of second type (Macdonald's function). Notice that the second term of the r.h.s of Equation (20) contains an explicit divergence in the factor $\Gamma(s-1/2) = \Gamma(-1)$ [34,35]. However, the derivative

in Equation (19) removes this issue. Thus, using Equation (20) to compute Equation (19), the Casimir energy results in

$$\mathcal{E}_C \approx \frac{\alpha}{2}\sqrt{\frac{b_0}{r_s-b_0}}\left[1+\frac{3}{4\sqrt{\pi}}\sum_{n=0}^{\infty}\frac{(-1)^n n\Gamma(n-3/2)}{n!}\left(\frac{b_0}{r_s-b_0}\right)^{1-n}(-1+2^{1-2n})\zeta(1-2n)\right], \tag{21}$$

where the factor outside the brackets is related to the zero-mode energy ω_0, and $\zeta[z]$ is the Riemann zeta-function. The last term of Equation (20) can be neglected since the Macdonald's function behaves asymptotically as a decreasing exponential of the argument (recall that $b_0/(r_s-b_0) \gg 1$).

Figure 4 shows the behavior of the Casimir force on each shell situated at symmetrical opposite sides nearby the wormhole throat (see the immersion diagram of Figure 5). The referred force can be computed as $\mathcal{F}_C = -\partial\mathcal{E}_C/\partial r_s$ and it is depicted as a function of the shell radius in tortoise coordinates, r_*^s. Notice that the force tends to expand the shells outwards to the wormhole throat. The Casimir force is bigger the bigger the parameter α is. On the other hand, the closer the shell is to the throat the stronger this force is. In fact, when $r_s \to b_0$ we have that $\mathcal{E}_C \approx (\alpha/4)\sqrt{b_0/(r_s-b_0)}$ and the following result arises

$$\mathcal{E}_C \approx \frac{2\alpha}{3}\left(\frac{b_0}{r_s-b_0}\right)^{3/2}+\frac{13\alpha}{24}\left(\frac{b_0}{r_s-b_0}\right)^{1/2}, \tag{22}$$

and the corresponding Casimir force reads

$$\mathcal{F}_C \approx \frac{\alpha e^{-\alpha r_*^s}}{6b_0}\left[\frac{e^{\alpha r_*^s}}{\left(e^{\alpha r_*^s}-1\right)^2}\right]^{5/2}\left(166e^{\alpha r_*^s}+13e^{2\alpha r_*^s}+13\right), \tag{23}$$

in tortoise coordinates.

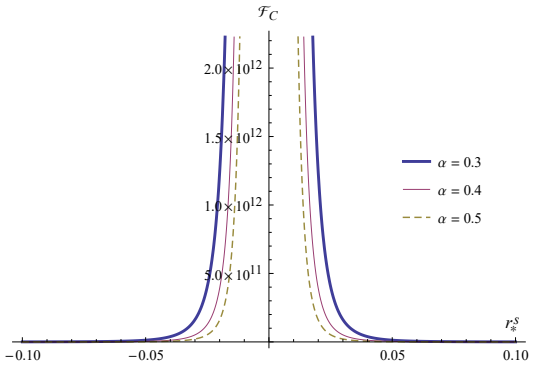

Figure 4. Casimir force on the thin material shells nearby the throat of a Rindler–Schwarzschild wormhole at its two opposite sides. The force is due to the vacuum of the massless scalar field obeying the Dirichlet boundary conditions, here depicted as a function of the shell radius in tortoise coordinates, r_*^s, for some values of α and for $b_0 = 1$, in Planck units.

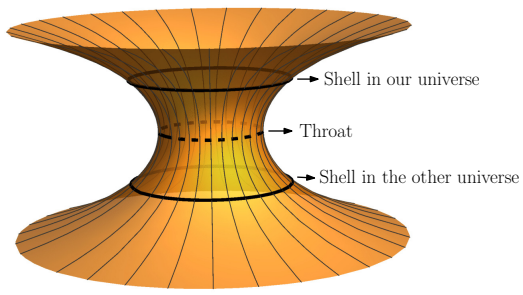

Figure 5. Immersion diagram of the deformed Schwarzschild-like wormhole, with the thin material shells nearby the throat at its two opposite sides.

6. Conclusions

In this paper we have studied the quantum relativistic features of a scalar field around the Rindler–Schwarzschild wormhole. Firstly, we presented this novel type of spacetime, which is asymptotically a Rindler spacetime. Then we investigated NEC and ANEC, verifying that these energy conditions are violated in a region nearby the wormhole throat, allowing us to compare these conditions with the ones obtained in Ref. [30] with respect to the Rindler–Ellis–Bronnikov wormhole. Regarding the NEC, we have also related our findings with those associated with the generalized Ellis–Bronnikov solution [31], where the violation region is even smaller. Thus, we conclude that our wormhole solution needs an exotic matter too, in order to prevent it from collapsing.

The study of the behavior of the massless scalar field around this spacetime permitted us to find the effective potential via tortoise coordinates transformation. We have shown that such a potential is attractive nearby the wormhole throat, and massive particles with low energies can quantum tunnel through it. Then we obtained the solution of the Klein–Gordon equation, showing that the energy of the field is subject to a constraint in order to present a decreasing oscillatory behavior. On imposing Dirichlet boundary conditions (b.c.) on a spherical shell nearby the throat, we determine the particle energy levels. Taking these data into account, we have calculated the quantum revival time, in other words, the minimum time necessary to the field return to this initial state. As a conclusion, we can say that this time decreases with the increase of the deformation parameter, α, and it increases with the increase of the quantum number ℓ of the particle.

Finally, we have computed the Casimir energy associated with the massless scalar field at zero temperature, by means of the sum of the modes method, taking into account the degeneracy of the system. Bt regularizing the obtained zero-point energy via the Epstein–Hurwitz zeta function, we have arrived at the Casimir energy, and then obtained the related force, as depicted in the Figure 4 as a function of the shell positions, in tortoise coordinates. We can then see that the force on the spherical shells placed on both sides of the throat, which tends to radially expand them, is bigger the smaller the deformation parameter is, α. We can also notice that such a force is more intense the closer the shells are to the throat; this feature is consistent with the fact that the presence of an exotic energy, such as Casimir, prevents the wormhole throat from collapsing.

Author Contributions: Conceptualization: C.R.M., H.R.C., M.S.C., J.F.; Methodology: C.R.M., H.R.C., M.S.C., J.F.; Software: C.R.M., M.S.C., J.F.; Validation: C.R.M., H.R.C., M.S.C., J.F., V.B.B.; Formal analysis: C.R.M., H.R.C., M.S.C., J.F., V.B.B.; Investigation: C.R.M., H.R.C., M.S.C. and J.F.; Writing draft preparation: C.R.M. and H.R.C.; Writing: C.R.M., H.R.C.; Review: C.R.M., H.R.C., M.S.C., J.F., V.B.B., Editing: C.R.M., H.R.C.; Visualization: C.R.M., H.R.C., M.S.C., J.F., V.B.B. All authors have read and agreed to the published version of the manuscript.

Funding: The authors thank the Conselho Nacional de Desenvolvimento Científico e Tecnológico (CNPq), grants nº 308268/2021-6 (CRM), 307211/2020-7 (VBB), and 315926/2021-0 (MSC) for the financial support.

Data Availability Statement: Not applicable.

Conflicts of Interest: The authors declare no conflict of interest.

References

1. Misner, C.W.; Wheeler, J.A. Classical physics as geometry: Gravitation, electromagnetism, unquantized charge, and mass as properties of curved empty space. *Ann. Phys.* **1957**, *2*, 525–603. [CrossRef]
2. Einstein, A.; Rosen, N. The Particle Problem in the General Theory of Relativity. *Phys. Rev.* **1935**, *48*, 73–77. [CrossRef]
3. Fuller, R.W.; Wheeler, J.A. Causality and Multiply Connected Space-Time. *Phys. Rev.* **1962**, *128*, 919–929. [CrossRef]
4. Bronnikov, K.A. Scalar-tensor theory and scalar charge. *Acta Phys. Polon. B* **1973**, *4*, 251–266.
5. Ellis, H.G. Ether flow through a drainhole—A particle model in general relativity. *J. Math. Phys.* **1973**, *14*, 104–118. [CrossRef]
6. Morris, M.S.; Thorne, K.S. Wormholes in space-time and their use for interstellar travel: A tool for teaching general relativity. *Am. J. Phys.* **1988**, *56*, 395. [CrossRef]

7. Morris, M.S.; Thorne, K.S.; Yurtsever, U. Wormholes, Time Machines, and the Weak Energy Condition. *Phys. Rev. Lett.* **1988**, *61*, 1446. [CrossRef] [PubMed]
8. Visser, M. Traversable wormholes: Some simple examples. *Phys. Rev. D* **1989**, *39*, 3182–3184. [CrossRef]
9. Dai, D.C.; Minic, D.; Stojkovic, D. How to form a wormhole. *Eur. Phys. J. C* **2020**, *80*, 1103. [CrossRef]
10. Dai, D.C.; Minic, D.; Stojkovic, D. New wormhole solution in de Sitter space. *Phys. Rev. D* **2017**, *98*, 124026. [CrossRef]
11. Shinkai, H.A.; Hayward, S.A. Fate of the first traversible wormhole: Black hole collapse or inflationary expansion. *Phys. Rev. D* **2002**, *66*, 044005. [CrossRef]
12. Bronnikov, K.A.; Krechet, V.G. Potentially observable cylindrical wormholes without exotic matter in general relativity. *Phys. Rev. D* **2019**, *99*, 084051. [CrossRef]
13. Gravanis, E.; Willison, S. 'Mass without mass' from thin shells in Gauss–Bonnet gravity. *Phys. Rev. D* **2007**, *75*, 084025. [CrossRef]
14. Richarte, M.G.; Simeone, C. Thin-shell wormholes supported by ordinary matter in Einstein-Gauss-Bonnet gravity. *Phys. Rev. D* **2007**, *76*, 087502; Erratum in **2008**, *77*, 089903. [CrossRef]
15. Eiroa, E.F.; Richarte, M.G.; Simeone, C. Thin-shell wormholes in Brans-Dicke gravity. *Phys. Lett. A* **2008**, *373*, 1–4; Erratum in **2009**, *373*, 2399–2400. [CrossRef]
16. Visser, M.; Kar, S.; Dadhich, N. Traversable wormholes with arbitrarily small energy condition violations. *Phys. Rev. Lett.* **2003**, *90*, 201102. [CrossRef] [PubMed]
17. Casimir, H. On the attraction between two perfectly conducting plates. *Proc. Kon. Ned. Akad. Wet.* **1948**, *51*, 793.
18. Sparnaay, M. Attractive forces between flat plates. *Nature* **1957**, *180*, 334. [CrossRef]
19. Sparnaay, M. Measurements of attractive forces between flat plates. *Physica* **1958**, *24*, 751. [CrossRef]
20. Lamoreaux, S. Demonstration of the Casimir force in the 0.6 to 6 μm range. *Phys. Rev. Lett.* **1997**, *78*, 5. [CrossRef]
21. Visser, M. *Lorentzian Wormholes: From Einstein to Hawking*; American Institute of Physics: New York, NY, USA, 1995.
22. Ford, L.H.; Roman, T.A. Quantum field theory constrains traversable wormhole geometries. *Phys. Rev. D* **1996**, *53*, 5496. [CrossRef]
23. Garattini, R. Casimir wormholes. *Eur. Phys. J. C* **2019**, *79*, 951. [CrossRef]
24. Muniz, C.R.; Christiansen, H.R.; Cunha, M.S.; Vieira, H.S. Exact solutions of the Wheeler–DeWitt equation with ordering term in a dark energy scenario. *Phys. Dark Universe* **2020**, *28*, 100547. [CrossRef]
25. Deng, H.; Garriga, J.; Vilenkin, A. Primordial black hole and wormhole formation by domain walls. *J. Cosmol. Astropart. Phys.* **2017**, *4*, 50. [CrossRef]
26. Bambi, C.; Stojkovic, D. Astrophysical Wormholes. *Universe* **2021**, *7*, 136. [CrossRef]
27. Mizuno, Y.; Younsi, Z.; Fromm, C.M.; Porth, O.; de Laurentis, M.; Olivares, H.; Falcke, H.; Kramer, M.; Rezzolla, L. The Current Ability to Test Theories of Gravity with Black Hole Shadows. *Nat. Astron.* **2018**, *2*, 585–590. [CrossRef]
28. Paul, S.; Shaikh, R.; Banerjee, P.; Sarkar, T. Observational signatures of wormholes with thin accretion disks. *J. Cosmol. Astropart. Phys.* **2020**, *3*, 55. [CrossRef]
29. Rindler, W. Kruskal space and the uniformly accelerated frame. *Am. J. Phys.* **1966**, *34*, 1174. [CrossRef]
30. Kar, S. Curious variant of the Bronnikov-Ellis spacetime. *Phys. Rev. D* **2022**, *105*, 024013. [CrossRef]
31. Kar, S.; Minwalla, S.; Mishra, D.; Sahdev, D. Resonances in the transmission of massless scalar waves in a class of wormholes. *Phys. Rev. D* **1995**, *51*, 1632. [CrossRef]
32. Elizalde, E. Five Physical Applications of the Inhomogeneous Generalized Epstein–Hurwitz Zeta Functions. In *Ten Physical Applications of Spectral Zeta Functions;* Lecture Notes in Physics; Springer: Berlin/Heidelberg, Germany, 2012; pp. 119–145. [CrossRef]
33. Elizalde, E. The vacuum energy density for spherical and cylindrical universes. *J. Math. Phys.* **1994**, *35*, 3308. [CrossRef]
34. Nesterenko, V.V.; Pirozhenko, I.G. Justification of the zeta function renormalization in rigid string model. *J. Math. Phys.* **1997**, *38*, 6265. [CrossRef]
35. Bezerra, V.B.; Mota, H.F.; Muniz, C.R. Casimir effect in the rainbow Einstein's universe. *Europhys. Lett.* **2017**, *120*, 10005. [CrossRef]